NUMERICAL STUDY OF THE TIME TO FAILURE OF GLASS UNDER STRESS CORROSION

H. AURADOU[1], D. VANDEMBROUCQ[2], C. GUILLOT[1] AND E. BOUCHAUD[1]

[1] Commisariat à l'Energie Atomique, Service de Physique et Chimie des Surfaces et Interfaces, Bât. 462, F-91191, Gif-sur-Yvette cedex, FRANCE
[2] Unité Mixte de recherche CNRS/Saint-Gobain "Surface du Verre et Interfaces", 39 quai Lucien Lefranc, F-93303 Aubervilliers cedex, FRANCE

ABSTRACT

The purpose of this paper is to examine the effect of a population of surface flaws on the time to failure of glass under static loading and subject to stress corrosion. The roughness of the glass surface is mapped onto a set of parallel elliptical cracks. The presence of the cracks modifies the stress field within the material and induces a shielding of the stress at the cracks tips which increases the lifetime of the material. We show that this effect becomes important when the length of the cracks is comparable to the distance separating them.

KEYWORDS

stress corrosion, surface flaws, glass, time to failure, shielding.

INTRODUCTION

An important practical problem is to predict the lifetime of a piece of glass under stress. The failure time depends upon the surface state, the loading and also on the environment. This delayed failure of glass is associated with *the stress-corrosion* growth of pre-existing tiny surface defects in the presence of humidity. The corrosion process has the important consequence that any (sufficient) stress tends to lengthen the flaw and that finally the object breaks after the flaw has reached a critical length. While the fundamental nature of these flaws remains unclear since it is difficult to observe them directly, the presence of surface defects has been clearly highlighted in various experimental conditions [1, 2, 3]. Mechanical contacts or thermal shocks can for example be responsible for surface cracks. However it is well known that freshly drawn fibers can be broken in a stress-corrosion regime while AFM studies could not reveal any flaw on their surface [4]. Later studies [5] showed that the nanometer scale roughness of the fiber surface presented long range correlations (up to 100nm); the surface is in fact self-affine

[6], meaning that it is statistically invariant under the transformation $x \to \lambda x$ and $z \to \lambda^H z$, where x is a distance in the mean plane of the surface and z a height difference. Here H is the Hurst exponent where $0 < H < 1$. Note that this very gentle roughness is responsible for fluctuations of the tangential stress at the surface, (see Ref.[7] for direct calculations of the stress field from the knowledge of the roughness *via* conformal mapping). In other words even if there is no evidence for flaws on the glass surface, there can be stress concentration effects due to the roughness. We, actually, propose in this work to map a rough surface onto a set of elliptical cracks distributed over a plane surface so that they are responsible for the same local stress concentrations. Then, we investigate the variations of the time to fracture due to the distribution of cracks. Moreover, we will consider that flaws are microcracks with atomically sharp tips which emerge normally at the external surface of the glass. Thus, we will not consider possible crack blunting [8, 9]. The glass is supposed to be perfectly elastic and submitted to constant remote tension. Due to the presence of neighboring cracks, the stress at the tip of each crack is altered and the cracks do not longer behave as isolated cracks. The following section describes the model used to take into account the cracks interactions in the growing process of the surface flaws.

DESCRIPTION OF THE MODEL

Initial configurations of the crack : We first start by considering a one dimensional self-affine profile with $H = 0.8$ consisting of M facets of size l when projected onto the horizontal plane. The lengths l and $L = Ml$ correspond respectively to the lower and the upper scales of the self-affine description. Furthermore, the average slope, s, of the facets are small enough to allow for the computation by conformal mapping [7] of the local stresses when the profile is considered under uniaxial tension σ_0. Since our interest focuses on the subpart of the profile where the stress is concentrated, parts of the profile where the stress is lower than σ_0 are removed from the computation. We then select from the remaining set of stress the local stress maxima i.e. parts of the profile where the stress is higher than the two closest remaining stresses. To each of the remaining stresses σ is associated an equivalent elliptical crack a long by l wide which is under a uniaxial stress σ_0. The length of the hole is chosen so that the stress at the tip of the major axis is the one obtained by the conformal mapping method *i.e.* $\sigma = \sigma_0(1 - 2a/l)$. The roughness of the profile is thus mapped onto a set of parallel elliptical cracks that emerge normally to the external surface. The average distance, b, between the cracks is of the order of few l and the cracks spread over a horizontal distance L. The self-affine profile generated is made of 20 to 200 facets and the final set of cracks typically contains from 5 to 50 cracks. The set of cracks is then reproduced by translation of constant steps L (periodic boundary conditions); the final crack configurations is thus a succession of identical sub-cracks set that contains cracks of various lengths.

Determination of the stress intensity factors : It is well known that the problem of a linear elastic solid with N cracks can be represented as a superposition of N problems involving one crack but loaded by unknown tractions induced by the other cracks and the remote loading; the so called *"pseudo tensions"* method [10, 11]. These tractions can be interrelated through a system of integral equations [12]. Recently, a simple and efficient technique to solve this problem based on the superposition technique and the idea of self-consistency applied to the average tractions on individual cracks has been proposed [13, 14]. The key assumption of the method is to decompose the stress on a crack into a mean part and a fluctuating part and to neglect the effect of the fluctuating stresses in the interactions. Thus the traction shed on a given crack by a second crack results from the uniform average traction on the second crack. This results in a major simplification of the problem, self-consistency imposing then to the averaged stresses to be the solution of a simple linear system. Other techniques using a

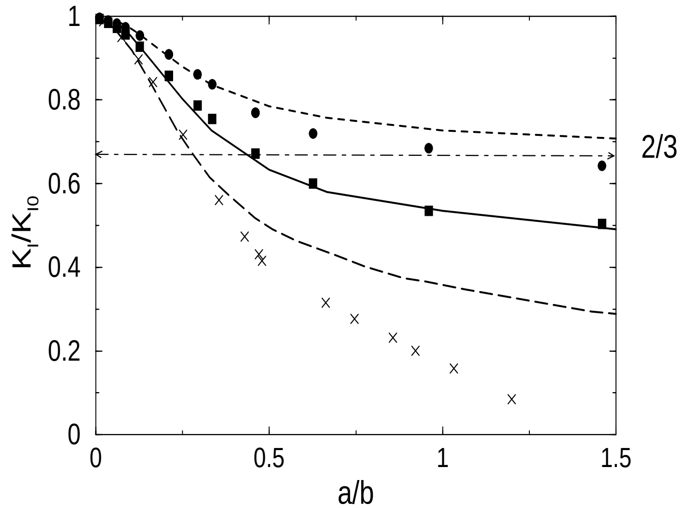

FIGURE 1. Curves of K_I/K_{I0} vs a/b for a semi infinite elastic plane containing a periodic array of N parallel cracks of same lengths a separated by a constant distance b and subjected to a uniform uniaxial stress σ_0 acting in a direction perpendicular to the cracks. $K_{I0} = 1.12\sigma_0\sqrt{\pi a}$ is the stress intensity factor for an isolated crack $N = 1$. Filled squares and filled circles represent the results obtained in our model for$N = 3$ cracks and correspond respectively to the inner and the outer cracks. The dashed and the solid lines show results from Isida [16]using a body force method for $N = 3$. The crosses show results obtained with our model for an infinite sequence of parallel cracks, these results are compared to the data of Bowie (long dashed line) [17].

polynomial approximation of the stress non-uniformities were also proposed [15], the method presented here is more efficient in terms of calculation time and was found sufficiently accurate.

Figure 1 compares results obtained by this method to other works[16, 17]. We see that while the ratio between the crack size and the distance between them is small enough, the results are in good agreement with previous works. Yet, discrepancy appears when the cracks length becomes of the order of the distance between them. This discrepancy comes from the fact that the non-uniformities of the tractions are not taken into account in our model. Moreover, it can be shown that the approach used is only valid for $K_I/K_0 > 2/3$; this lead to a major restriction on the ratio between the crack length a and the distance between them b which has to be less than unity.

Crack propagation law : From the experimental studies [8, 18, 19, 20], it is clear that crack velocity is strongly affected by the stress assisted corrosion reaction between the glass and the corrosive species in the atmosphere. Moreover, it appears that the velocity is uniquely related to the stress intensity factor. Depending on the stress intensity factor, three different regions are observed. In our work we mainly focus on the so called Region I which corresponds to the low speed regime. In this domain, the speed of the crack typically lies between $10^{-10}$and $10^{-5}m.s^{-1}$. In the other regions, crack propagation is fairly rapid and the range of stress intensity factors involved is narrow. Thus for long enough test times the contribution to the time before rupture in these regions is negligible.

Wiederhorn *et al* [19] carefully studied the low speed domain of the crack growth for various glasses and various environmental conditions. The data were found to fit the equation :

$$v(K_I) = v_0 exp(\frac{-E^* + cK_I}{RT}), \tag{1}$$

where $v(K_I)$ is the crack velocity, T the temperature. $E^*$is the apparent activation energy at zero load and c is the stress intensity factor coefficient. In this work we set the activation energy to zero. This has the consequence that under any applied stress, all the cracks are allowed to grow independently of their length. By normalizing the speed by the speed v_0 of the cracks at small stress intensity factor, equation 1 becomes :

$$v(K_I) = exp(c^* K_I) \tag{2}$$

with $c^* = c/RT$. The different steps of the simulation can be summarized as follows. We first compute the initial crack configuration. Using the method described in **??**, the stress intensity factor at the tip of each crack is calculated. The speed of each of the cracks is obtained using the crack growth law chosen (Eq. 1). The length of each crack is then incremented by $\Delta a = v(K_I)\Delta t$ where Δt is a fixed time step. The computation of the stress intensity factors and the crack growth are iterated until one of the cracks reaches the critical stress intensity factor K_{Ic} above which failure of the sample occurs. The lifetime of the material is defined as the time needed by the crack that reaches K_{Ic} the first to grow from its initial size to its final length.

In the following, we will study the effect of the cracks interactions on the life time of the material. We will first consider a single crack configuration.

QUALITATIVE DESCRIPTION OF THE CRACK GROWTH

Figure 2 shows, for a single crack configuration, the evolution of the ratio between the stress intensity factor for each of the cracks and the stress intensity factor of the cracks when considered as isolated. For small cracks size, which corresponds to the beginning of the simulation, the ratio of the stress intensity factors is close to one, meaning that each crack can be seen has isolated. But while the crack length increases, this ratio decreases until one of the cracks is long enough so that K_{Ic} is reached and that fracture occurs. We see from this example that the presence of a neighbourhood of cracks results in a decrease of the stress intensity factors. Due to this shielding effect, the speed of each crack is lower than what it would have been in the absence of shielding. The progression of the cracks is thus slowed down and as a consequence the lifetime of the material increases. Here the increase of the lifetime is of the order of 35%. When the shielding effect is absent and since the longest crack has the highest velocity, it is always this crack that reaches K_{Ic} the first. But it has to be pointed out that for some crack configurations, the shielding on the longest crack can be strong enough so that another crack which was not intially the longest one reaches K_{Ic} the frist. The shielding effect, thus, strongly depends on the initial cracks configuration. In the next section, we investigate the effect of the statistical distribution of the crack lengths on the lifetime of the material.

QUANTITATIVE RESULTS

Depending on the self-affine profile generated, different crack configurations can be obtained. These configurations differ in the the crack lengths and also in the arrangement of these cracks and, thus, each configuration will lead to a different lifetime.

Figure 3 shows the distribution of the ratio between the lifetime and the lifetime of the material when the longest crack is considered as isolated. We see that the times ratios are always larger than 1, meaning, as discussed previously, that the interactions between the cracks increase the life time of the material. Configurations obtained using $s = 0.1$ give rise to a broad distribution of lifetimes which gets sharpes when s decreases.

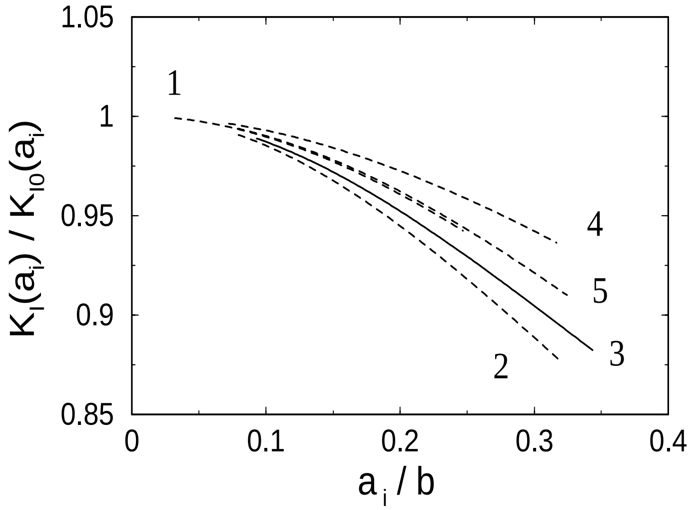

FIGURE 2. Evolution of the stress intensity factor for a single crack configuration as a function of the length a_i of crack i. A self-affine profile with roughness exponent $H = 0.8$ made of $M = 15$ facets of average slope $s = 0.1$ under uniaxial tension $\sigma_0 = 1$ is used to generate the configuration made of 5 cracks. Here, the relationship between the speed of the crack and the stress intensity factor is : $v(K_I) = exp(K_I)$ and $K_{Ic} = 1$. b is the distance between the cracks. $K_I(a_i)$ is the stress intensity factor of the crack i when cracks interact. $K_{I0}(a_i) = 1.12\sigma_0\sqrt{\pi a_i}$ corresponds to the stress intensity factor of an isolated crack of length a_i .

This effect is mainly due to the change in cracks lengths when the self-affine profile generated gets smoother. In fact, a decrease of the facets slope changes the length of the cracks that shrinks and as a consequence the ratio between the crack length and the distance separating them is decreased. For the configurations studied, the average crack length referred to the distance separating them is $< a > /b = 8.10^{-2}$ when the facets slope s is 0.1, while for $s = 0.01$ this ratio is 8.10^{-3} and drops to 8.10^{-4} when $s = 0.001$. As shown in the previous section, this will deeply influence the shielding effect, that has less influence on the growing process when the ratio $a/b << 1$.

For small $< a > /b$, the cracks grow as if they were isolated, and as a consequence the lifetime of the material is close to the time to failure without shielding. When $< a > /b$ becomes large enough, the shielding effect becomes important and this has a strong effect on the life time which can be quite larger than the life time without interaction.

CONCLUSION

We have developed a model of crack growth where the modification of the stress field due to the presence of neighboring cracks is taken into account. Our model allows for the computation of the stress intensity factors of a set of parallel sharp surface cracks submitted to tensile stresses. This model has been applied to stress corrosion growth of pre-existing surface flaws. The initial flaw configuration is obtained by mapping the self-affine roughness of the external surface of the glass considered under tension onto a set of parallel elliptical cracks. The growing rate of each crack is uniquely related to its stress intensity factors by a relation that fits previous experimental works. We have shown that the presence of neighboring cracks lead to a shielding of the stresses at the tip of the cracks and to an increase of the time to failure. Moreover this increase of the lifetime becomes non negligible when the shielding effect is important. This is

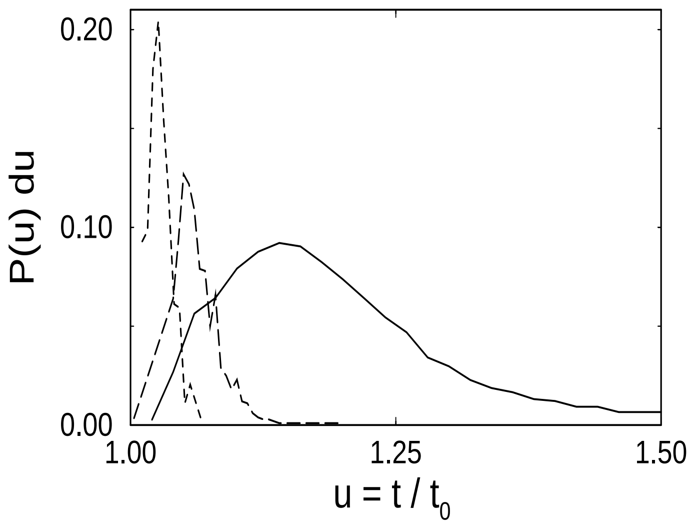

FIGURE 3. Distribution of the ratio of lifetime, t, when interaction are taking into account to the lifetime, t_0, in the absence of interactions. The data were obtained using 600 initial crack configurations generated using self-affine profiles made of facets of different slopes s. Solid, dotted and long dashed lines correspond respectively to $s = 0.1$, 0.01 and 0.001. The crack velocity law used is $v(K_I) = exp(K_I)$ and $K_{Ic} = 1$.

achieved when the crack lengths become of the order of the distance separating them. We have, also, pointed out that, due to shielding and depending on the crack configuration, others cracks than the longest can lead to the failiure of the sample. The effect of the remote tension an the lifetime has been studied also and it appears that the shielding effect has a strong influence on the lifetime when the remote tension is decreased. Further work is presently carried on to characterize the distribution of lifetime in terms of a Weibulh distribution.

REFERENCES

[1] da C. Andrade, E.N. and Tsien, L.C. (1937) *Proc. Roy. Soc.* A. 159, 346.
[2] Poloniecki, J.D. and Wilshaw, T.R. (1971) *Nature Physical Science* **229**, 226.
[3] Adams, R. and McMillan, P.W. (1977) *J. Mat. Sci.* **12**, 2544.
[4] Guilloteau, E. (1997), PhD Thesis, University Paris XI, France.
[5] Nghiêm, B. (1998). PhD Thesis, University Paris VI, France.
[6] J. Feder, Fractals, Plenum press, (1988).
[7] Vandembroucq, D. and Roux, S. (1997) *Phys. Rev. E.* **55** [5] 6186.
[8] Crichton, S.N. and Tomozawa, M. (1999) *J. Am. Ceram. Soc* **82** [11] 3097.
[9] Bando, Y., Ito, S. and Tomozawa, M. (1984) *J. Am. Ceram. Soc.* **67** [3] C36.
[10] Gong S.X. and Horii, H. (1989) *J. Mech. Phys. Solids* **37** (1), 27.
[11] Hori, M. and Hemat-Nasser, S. (1987) *J. Mech. Phys. Solids* **35** (5), 601.
[12] Datsyshin, A.P. and Savruk, M.P. (1973) *J. Appl. Math. Mech.* **37**, 306.
[13] Kachanov, M. (1985) *Int. J. Fracture* **27**, 113.
[14] Kachanov, M. and Montagut, E. (1986) *Eng. Frac. Mech.* 25, 625.
[15] Chudnovsky, A. and Kachanov, M. (1983) *Int. J. Engng. Sci* **21**, 1009.
[16] Isida, M. (1979) *Trans. Japan Soc. Mech. Engrs.*,**45** [392], 306.
[17] Bowie, O.L. (1972). In:*Method of analysis and solutions of crack problems*, ed. by G.C. Sih, Noordhof Int. Pub. Vol. I.
[18] Wiederhorn, S.M. (1967) *J. Am. Ceram. Soc* **50** [8], 407.
[19] Wiederhorn, S.M. and Bolz, L.H. (1970) *J. Am. Ceram. Soc* **53** [10], 543.
[20] Lawn, B.R., Jakus, K. and Gonzalez, A.C. (1985) *J. Am. Ceram. Soc.* **68** [1], 25.